Characterization of textural failure mechanics of strawberry fruit

Xue An[1,4], Zhiguo Li[1,4,*], Manuela Zude-Sasse[2], Fideline, Tchuenbou-Magaia, [3], Yougang Yang[1]

[1]*College of Mechanical and Electronic Engineering, Northwest A&F University, Yangling, 712100, China*

[2]*Department of Horticultural Engineering, Leibniz Institute for Agricultural Engineering and Bioeconomy, D-14469, Potsdam, Germany*

[3]*School of Engineering, Division of Chemical Engineering, University of Wolverhampton, Wolverhampton, WV1 1LY, United Kingdom*

[4]*Key Laboratory of Agricultural Internet of Things, Ministry of Agriculture and Rural Affairs, Yangling, 712100, China*

[*]*Email:lizhiguo0821@163.com Tel/Fax: +86-29-87092391*

Abstract

Fresh strawberry fruit is highly susceptible to damage during mechanical handlings. To prevent fruit macro-damage from external forces and predict damage evolution in internal tissues, the textural failure mechanics of strawberry fruit and its tissues were characterized by loading-unloading tests at different compression speeds. Strawberry fruit showed expected three stages of deformation during the loading phase, namely elastic, local plastic and structural failure deformation. Their cut-off points depended on the compression speed and loading direction, which was validated further by the corresponding visible browning processes in tissues from fruit longitudinal equatorial section. The peak force and absorbed energy depended on the loading direction and compression speed while the percentage of damaged mass only depended on the loading direction. The fruit was most susceptible to mechanical damage when it was compressed along its stem-blossom axis at low percentage deformation and along its radial axis at high percentage deformation. The absorbed energy and percentage of damaged mass of the strawberry fruit was correlated, which suggested that the absorbed energy could be an appropriate and easily measurable mechanical parameter for quantitatively assessing the degree of fruit damage. The failure stress, failure energy and elastic modulus of fruit tissues increased with the compression speed, while this factor did not affect the failure strain. The average failure stress, failure strain, failure energy and elastic modulus of fruit inner tissue were 0.093 MPa, 17.7%, 8.09 mJ, 0.53 MPa, which was 1.27, 1.14, 1.47, 1.15 times enhanced compared to values of outer tissue (p<0.05), respectively.

Keywords: strawberry fruit; brown tissue; failure mechanics; elastic modulus; percentage of damaged mass.

1. Introduction

Fresh strawberry (*Fragaria* × *ananassa* Duch.) is an important component of many human diets and its annual production is more than 198 thousand tons with a gross production value more than 12.3 billion dollars since 2010 (FAOSTAT, 2019); therefore, its quality is also economically crucial (Bovi et al., 2018). Texture is one of the most critical quality attributes in consumer evaluation of fresh fruit and vegetables (Sirisomboon et al., 2012). Strawberries are very susceptible to damage during mechanical handlings resulting in high perishability and handling requirements to avoid loss of quality (Liang et al., 2020). Losses begin at the farm and accumulate throughout the supply chain (Kelly et al., 2019; La Scalia et al., 2016), since mechanical damage may lead to accelerated deterioration of a whole fruit during subsequent handling (Li and Thomas, 2014). Many fruits with apparently little damage during harvesting are subsequently discarded in the harvest-consumption chain, which result in food wastage and seriously affects the economic benefit of sellers (Li and et al., 2019; Tang et al., 2019; Zhuang et al., 2018). From a material science viewpoint, fruit mechanical damage is a failure behavior of living tissue or internal structure when a fruit is subjected to excessive tension, compression or shear forces (Li et al., 2017a), and as such, it is closely dependent on fruit textural mechanics. The fruit mechanics will be a vital basis for assessing postharvest fruit quality (Chaves et al., 2017; Contigiani et al., 2018; Duarte-Molina et al., 2016), predicting internal mechanical response (e.g. damage evolution) under different handling processes (Li, 2013; Li et al., 2017b), and developing mechanical handling equipment (e.g. harvesting robot fingers, washing, grading and packing machines) (Ji et al., 2017; Mahalik and Nitaigour, 2014).

Previous research on strawberry textural mechanics can be classified into two aspects related to the postharvest conditions and its impact on fruit damage and the textural change during fruit development and in shelf life. An early study illustrated that fresh '*Selva*' strawberries were graded as unsaleable if the skin has serious abrasions or bruises penetrating deeply into the surface after vibration treatments. Furthermore, it was found that more than 50 % strawberries subjected to 7.5~10 Hz vibrations in the top box were unsaleable (Aliasgarian et al., 2015). Chaiwong and Bishop (2015) reported that the vibration frequencies ranging from 3~5 Hz affected the quality of '*Elsanta*' strawberry as described by its electrical conductivity which is associated with the severity of the bruises. The authors also found that the vibration at 5 Hz for 150 sec was the critical condition for the

increase of fruit loss. Aliasgarian et al. (2015) illustrated that the maximum damage of '*Gaviota*' strawberries was found during delivery at the bottom rows in the boxes. Similarly, the mechanical damage was influenced by the position of the box inside the truck with more damage in boxes at the higher position. Kelly et al. (2019) proposed that maintaining a constant optimum temperature throughout the supply chain is paramount to reducing strawberry quality losses and consequently waste. Consistently, varying temperatures during postharvest handling such as storage at the grower at 5 °C, shipping to the stores at 8 °C, and storage at the consumer level at 20 °C had the greatest impact on overall strawberry quality, e.g. firmness.

More fruit quality-related researches focused on the firmness change of strawberries in postharvest. Some literatures demonstrated that the firmness of strawberry mainly depended on fruit cultivar (Aliasgarian et al., 2015; Pham and Liou, 2017; Zeliou et al., 2018), storage time and condition (La Scalia et al., 2016) and fresh-keeping method (Contigiani et al., 2018; Yan et al., 2019; Zhang et al., 2018), whereas the vibration frequency had no impact on firmness (Chaiwong and Bishop, 2015; Dieter Fischer, 1990). Contigiani et al. (2018) showed an approximately linear increase of stress with the strain up to the epidermis rupture point when strawberry fruit was punctured at 30 mm/min and the epidermis contributed approximately 50-55% to the firmness of the fruit before the rupture force, and the rupture force of fresh '*Albion*' strawberries was 2.4~3.1 N. Ozonized water washing for 5 min along with cold storage can extend the strawberry shelf-life by decreasing fungal decay and water loss while the storage time and crop year had a significant effect on the fruit mechanics. In contrast, modified atmosphere packaging could potentially affect fruit's development and firmness (Contigiani et al., 2018). Zhang et al. (2018) demonstrated that the firmness of fresh strawberry packaged with permeable films decreased with increasing storage time, but the decrease was delayed compared to control fruit measured using puncture tests at 2 mm/s. Similarly, Yan et al. (2019) concluded that edible coating had a positive effect on the maintenance of fruit firmness in '*Akihime*' strawberry; The firmness of strawberry coated by e.g. 1% chitosan affecting the gas permeability and viscoelastic properties was about 0.4 N higher than the uncoated fruits after eight days of storage measured by puncture test at 0.5 mm/s.

Nevertheless, closer information on the textural failure mechanics of strawberry fruit and its tissues under different loading conditions, e.g., different compression speeds, loading directions, and percentage deformations, are still missing. Consequently, it is difficult to quantitatively assess the

internal mechanical damage evolution and damage volume changing of strawberries by numerical simulation. This gap also hampers the development of non-destructive methods for fruit quality analysis (Zude et al., 2006, 2019) and limit the opportunities for investigating the effects of the application of external forces during harvesting (Zhuang et al., 2019), packaging and transport for recommending improved handling methods in the supply chain (Li et al., 2017b; Li and Thomas, 2014). The objectives of this study were, therefore (i) to compare the mechanical deformation behavior of strawberries at different compressibility levels; (ii) to test the effects of compression speed and loading direction on the textural failure mechanics of strawberries at different percentage deformation by loading-unloading tests; and (iii) to characterize the failure mechanics of strawberry fruit's outer and inner tissues by loading-unloading tests at different compression speeds.

2. Materials and methods

2.1 Materials

'*Hongyan*' strawberries were grown in a greenhouse at the Yangling Agricultural Hi-tech Industries Demonstration Zone, China. 220 fresh fruits were manually harvested in May 2019 at the bright-red ripening stage proposed by Ornelas-Paz et al. (2013). In the laboratory, the fruit surfaces were manually cleaned with water and dried naturally under ambient air (22 ± 1˚C). All the samples were cool-stored at about 4˚C before testing. The tests were performed within 48 h, on fruits that were allowed to reach room temperature (22 ± 1˚C, 50-55% RH). Note that strawberries and strawberry fruits are used interchangeably in this paper.

2.2 Determination of fruit physical properties

Firstly, 180 strawberry fruits were randomly sorted into four groups and labeled. Each fruit was placed on an inverted plastic cylindrical cap on the table with its stem-blossom axis parallel to the table surface (Fig. 1a). Subsequently, the fruit was photographed with a digital camera from its top (top view) and was then counterclockwise rotated 90° along its stem-blossom axis for repetitive photographing from its top (side view). In total, 360 images were taken. The captured images were transmitted to the computer and processed (Digimizer image analysis software 4.3.4, MedCalc Software, USA) for extracting three principal dimensions: the longitudinal height H, major transverse diameter D_1 and minor transverse diameter D_2 (Fig.1a). The major and minor transverse diameters indicate the maximum diameter of a fruit on the transverse equatorial section and the corresponding orthogonal diameter, respectively. Finally, the geometric mean diameter GMD, sphericity Ø and

surface area S were calculated (Equations 1-3) (Jahanbakhshi et al., 2018). The fresh mass m_1 of each fruit was measured by a JCS-A electronic balance (Kaifeng Group Co., Ltd., China) with the accuracy of 0.01 g. The bulk density ρ_1 of strawberry tissues was measured by a MH-300A automatic density measuring instrument (Xiamen Fubusi Testing Equipment Co., Ltd., China) with the accuracy of 0.001 g/cm^3.

$$GMD = (HD_1D_2)^{1/3} \quad (1)$$

$$\emptyset = \frac{(HD_1D_2)^{1/3}}{H} \quad (2)$$

$$S = \pi(HD_1D_2)^{2/3} \quad (3)$$

where H- longitudinal height of the fruit, cm; D_1 and D_2- major and minor diameter of the fruit on its transverse equatorial section, respectively, cm; GMD-geometric mean diameter of the fruit, cm; $\emptyset$-sphericity of the fruit; S-surface area of the fruit cm^2.

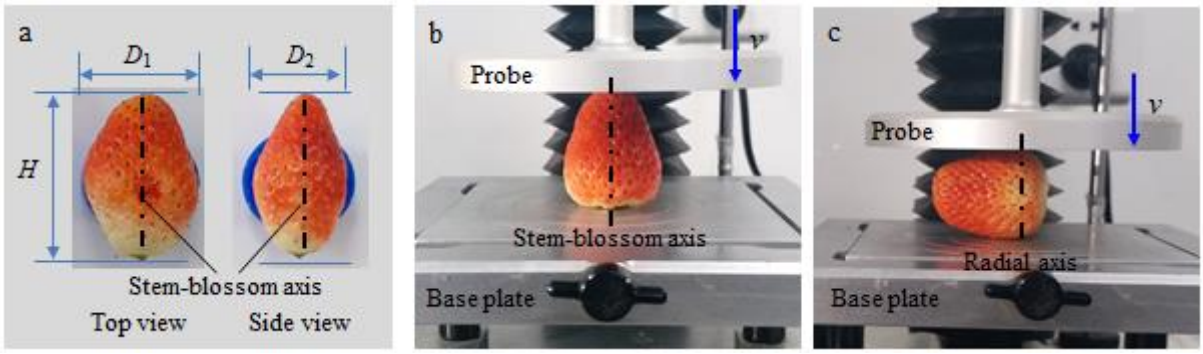

Fig.1 Loading-unloading test of strawberries (a) Top and side views of a strawberry fruit; (b) Compression along the stem-blossom axis on the fruit longitudinal equatorial section; (c) Compression along the radial axis on the fruit transverse equatorial section.

2.3 Determination of whole fruit failure mechanics

A full factorial design was performed, consisting of two loading directions along the stem-blossom axis on the fruit longitudinal equatorial section (Fig. 1b) and the radial axis on the fruit transverse equatorial section (Fig. 1c), two compression speeds (1 mm/s and 5 mm/s) and nine compressibility levels (0, 2.5%, 5%, 7.5 %, 10%, 15%, 20%, 40% and 60%). In total, 180 strawberry fruits (5 samples × 2 compression speeds × 2 loading directions × 9 compressibility levels) were placed on the base plate for loading-unloading tests. Each fruit was compressed to the compressibility level between the metal base plate and the moving flat-end probe of a TA-XT plus Texture Analyzer (Stable Micro Systems Ltd., UK). The analyzer was calibrated with a 5 kg weight before the first test.

The probe consisted of a plate with 100 mm diameter, which moved 10 mm to the fruit surface during each measurement. The experimental force - deformation curve was recorded in real-time. Subsequently, the peak force (F_p), loading slope (k), and absorbed energy (E_a) were extracted from each curve recorded. Furthermore, after a group of samples were tested with orientation along their stem-blossom axis or along their radial axis on the fruit transverse equatorial section, each fruit in the group was cut into halves immediately along its stem-blossom axis or radial axis and parallel to its stem-blossom axis. The resulting samples were placed on a table for enzymatic browning for 4 hours. The fruits with 0 % compressibility level were regarded as a control group, and their fresh masses m_0, and after storage (22 ± 1˚C, 50-55% RH) for 4 hours masses, m_0', were measured using the JCS-A electronic balance (Kaifeng Group Co., Ltd., China). The ratio η of water loss during the exposure to air for 4 hours for the control group was calculated using Equation (4). Subsequently, the browning tissue in each fruit sample was removed using a dissecting needle and a R35 disposable microtome blade. The mass m_3 of the other non-browning tissue in the fruit sample was also measured. It was hypothesized that the browning tissue in fruit corresponded to the damaged tissue during compression and the other non-browning tissue associated with the non-damaged tissue. Moreover, it was assumed that the compressed fruit in a group have the same water loss rate in the first 4 hours after cutting open. Hence the mass m_4 of the damaged tissue in each fruit sample and its corresponding percentage damaged mass R was calculated using Equations 5-6. The reported values of all fruit failure mechanical parameters were means of 5 replicates.

$$\eta = \frac{m_0 - m_0'}{m_0} \tag{4}$$

$$m_4 = m_1 - m_2 - m_3 = m_1 - m_1\eta - m_3 \tag{5}$$

$$R = \frac{m_4}{m_1} \times 100\% \tag{6}$$

where η - ratio of water loss of the fresh fruit in the control group; m_0 and m_0'- fresh mass initially and after storage for 4 hours' mass of the fruit in the control group, g; m_1 - initial mass of a fresh fruit in the experimental group, g; m_2 - mass of water loss in a compressed fruit after 4 hours' storage, g; m_3 - mass of non-damaged tissue in a compressed fruit after 4 hours' storage, g; m_4 - mass of damaged tissue in a compressed fruit after 4 hours' storage, g; R-percentage damaged mass of tissue in a compressed fruit after 4 hours' storage, %.

2.4 Determination of tissue failure mechanics

Each fruit (n = 40) was cut into halves with a sharp knife along its stem-blossom axis on the fruit longitudinal equatorial section (Fig. 2a). Because the rectangular block samples are easy for applying a normal force in perpendicular to the base plate (Pérez-López et al., 2014) and there might be differences in mechanics between outer and inner tissue (Fig. 2a), some standard rectangular outer and inner tissue blocks were prepared for loading-unloading tests using a R35 disposable microtome blade. Subsequently, each tissue block was photographed with a digital camera from its top and side. The captured images were processed by commercial software (Digimizer image analysis 4.3.4 MedCalc Software, USA) for extracting sample's length L, width w and thickness d. The mechanical properties of two types of strawberry tissue samples were determined by the calibrated TA-XT plus Texture Analyzer with one-dimensional compression tests at three different compression speeds: 1 mm/s, 3 mm/s and 5 mm/s based on the National Standard GB/T 7314-2017. The compressibility level was set to 50%. Each prepared tissue sample was put on the center of the base plate and was compressed along its length direction by a P50 plate probe (Fig. 2b). The force-deformation data were recorded by a computer in real-time. Lastly, the mechanical parameters of strawberry tissues such as elastic modulus E_c, failure stress σ_c, failure strain ε_c and failure energy E_{rec} were derived using Equations 7-10 (Li et al., 2012; Stopa et al., 2018). In total, 30 strawberry tissue samples (5 samples × 2 tissue types × 3 compression speeds) were tested. The reported values of all tissue mechanical parameters were means for 5 replicates.

$$\sigma_c = \frac{F_{c\,max}}{A_c} = \frac{F_{c\,max}}{wd} \tag{7}$$

$$\varepsilon_c = \frac{\Delta L}{L} \tag{8}$$

$$E_c = \frac{\sigma_c}{\varepsilon_c} \tag{9}$$

$$E_{rec} = \int_0^{\Delta L} F d\Delta L \tag{10}$$

where σ_c - failure stress of the tissue, MPa; $F_{c\,max}$ - elastic peak force, N; A_c - cross sectional area of the sample, mm^2; w - cross sectional width of the sample, mm; d-cross sectional thickness of the sample, mm; ε_c - failure strain of tissue, %; ΔL - the difference in length of the sample before and after test, mm; L - initial length of the sample, mm; E_c - compression elastic modulus, MPa; E_{rec} - failure energy, mJ; F - compression force, N.

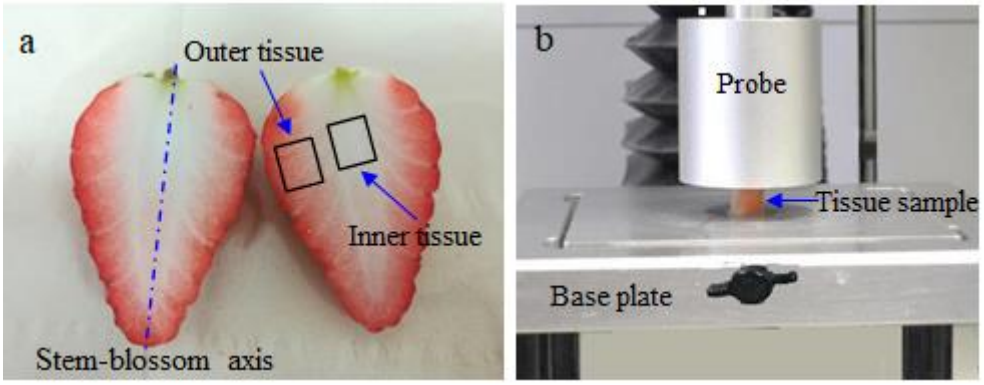

Fig.2 Loading-unloading test of strawberry tissue samples. (a) sampling of outer and inner tissues, (b) compression test of a tissue sample.

2.5 Statistical analysis

Multivariate analysis of variance (MANOVA) and Pearson correlation analysis were performed using SAS software, version 9.2 (SAS Institute Inc., Cary, NC, USA). The Fisher's least significant difference method was used for multiple comparison tests in MANOVA. The significance level was set at 0.05.

3. Results and discussion

3.1 Physical properties

The loading directions along the stem-blossom axis on the fruit longitudinal equatorial section and along the radial axis on the fruit transverse equatorial section and two compression speeds (1 and 5 mm/s) were included in the design of experimental factors, resulting in four groups of samples according to compression speed × loading direction (Table 1). The geometric mean diameter, sphericity, surface area, fresh mass and density of strawberry fruit samples varied from 3.44 to 3.56 cm, 0.84 to 0.86, 37.52 to 40.22 cm^2, 12.31 to 12.97 g, and 1.005 to 1.018 g/cm^3, respectively. No difference in each physical parameter was found between the four groups at the significance level 0.05 according to MANOVA. This indicates that the original four fruit sample groups were well-balanced and did not bias the data obtained by the loading-unloading tests because of distinct fruit physical characteristics associated with each compression speed or loading direction test group.

Table 1 Physical properties of strawberries

Parameters	Loading along the stem-blossom axis		Loading along the radial axis	
	1 mm/s	5 mm/s	1 mm/s	5 mm/s
GMD, cm	3.44±0.35[a]	3.49±0.27[a]	3.56±0.34[a]	3.53±0.32[a]

Φ	0.86±0.05[a]	0.84±0.04[a]	0.84±0.05[a]	0.85±0.05[a]
S, cm^2	37.52±7.80[a]	38.40±5.90[a]	40.22±7.60[a]	39.50±7.20[a]
m_1, g	12.31±3.49[a]	12.34±2.39[a]	12.97±2.87[a]	12.76±3.21[a]
ρ, g/cm^3	1.018±0.035[a]	1.005±0.002[a]	1.016±0.021[a]	1.007±0.029[a]

Note: Data are expressed as the mean ± standard deviation (n = 40). Different superscript letters (namely a, b) in the same row indicate significant difference ($p < 0.05$) according to MANOVA. *GMD*, Φ, S, m_1, and ρ - geometric mean diameter, sphericity, surface area, fresh mass and density of strawberry fruit samples, respectively.

3.2 Failure mechanical behavior of whole strawberries

3.2.1 Loading-unloading tests

Figure 3-a1 shows eight typical force-percentage deformation curves in the uniaxial loading-unloading tests and corresponds to the force-percentage deformation data of eight strawberry fruit samples compressed to a given compressibility level (e.g., 2.5 %, 5 %, 7.5 %, 10 %, 15 %, 20 %, 40 % and 60 %) along its stem-blossom axis at 1 mm/s, respectively. Each force-percentage deformation curve included a loading phase and an unloading phase. Fig. 3-a2 and a3 show the browning tissues on the fruit longitudinal equatorial section after the fruit samples were compressed to a given percentage deformation at 1 and 5 mm/s and then stored for 4 h. When the compressibility level was 2.5 %, the loading phase in each force-percentage deformation curve approximated linear (Fig. 3-a1) and no visible browning was recognized on the fruit longitudinal equatorial section (Fig. 3-a2 and a3), thus, 2.5 % could be regarded as the elastic deformation limit of fruit along the compression direction of stem-blossom axis at 1 and 5 mm/s. The loading phase of some force-percentage deformation curves showed an obvious inflection point which after analysis was found to correspond to the percentage deformation of fruit samples, 20.9 ± 9.5 % at 1 mm/s and 20.1 ± 3.8 % at 5 mm/s, respectively. Before each inflection point, the loading phase in each force-percentage deformation curve appeared linear (Fig. 3-a1), while clearly, visible tissue browning started to occur on the longitudinal equatorial section of each fruit sample, and the size of browning area gradually increased with fruit deformation (Fig. 3-a2 and a3). Consequently, 2.5~20.9 % and 2.5~20.1 % could be regarded as the local plastic deformation ranges of fruit samples along the loading direction of the stem-blossom axis at 1 and 5 mm/s, respectively. After the inflection point was reached, the

compression resulted in no further static linear response of force to percentage of deformation and the loading force inclined with the increasing fruit percentage deformation, followed by slight ascending in the loading phase (Fig. 3-a1). On the other hand, the browning degree on the longitudinal equatorial section of each fruit sample rapidly increased with fruit deformation (Fig. 3-a2 and a3), thereby indicating the presence of an internal structural fracture in the fruit samples from the inflection point. Hence, 20.9 % and 20.1 % was regarded as the initial percentage deformation of fruit samples having an internal structural failure when the fruit samples were compressed along its stem-blossom axis at 1 and 5 mm/s, respectively.

The eight typical force-percentage deformation curves of fruit samples compressed to a given compressibility level (2.5 %, 5 %, 7.5 %, 10 %, 15 %, 20 %, 40 % and 60 %) along their radial axis on the transverse equatorial section at 1 mm/s are shown in Figure 3-b1. After the fruit samples were compressed to a given percentage deformation at 1 and 5 mm/s and then stored for 4 h, their browning tissues on the longitudinal equatorial sections are presented in Fig. 3-b2 and b3, respectively. The findings were similar to the compression along the fruit stem-blossom axis where 2.5 % deformation was regarded as the elastic deformation limit of fruit at the compression speeds of 1 and 5 mm/s. However, the inflection points in the loading phase of some force-percentage deformation curves corresponded to the percentage deformation of fruit samples, 28.1 ± 4.4 % at 1 mm/s and 32.9 ± 7.5 % at 5 mm/s, respectively. Hence, 2.5~28.1 % and 2.5~32.9 % could be regarded as the local plastic deformation ranges of fruit samples at the loading direction of the radial axis on the fruit transverse equatorial section at 1 and 5 mm/s, respectively. At the upper threshold, 28.1 % and 32.9 % could be considered as the limit for percentage deformation of fruit samples causing an internal structural failure when samples were compressed along their radial axis at 1 and 5 mm/s, respectively. When the compressibility level was less than 28.1 % at 1 mm/s or 32.9 % at 5 mm/s, the browning area gradually increased with percentage fruit deformation (see the first six images of Fig. 3-b2 and b3 showing the browning area). Conversely, there was a rapid increase in tissues browning area on the longitudinal equatorial section of each fruit sample when the compressibility level reached more than 28.1 % at 1 mm/s or 32.9 % at 5 mm/s as illustrated by the last two images of Fig. 3-b2 and b3.

To sum up, taking the force-percentage deformation curve of fruit with 60 % percentage deformation as an example, the loading phase *OC* included three parts, namely *OA* – fruit elastic deformation, *AB* – fruit local plastic deformation and *BC* – fruit structural failure. The peak force F_p

corresponds to the force at the first significant peak point where the force falls off during loading phase and the loading slope *k* is the slope of the first part *OA* in the loading phase of the corresponding force-deformation curve. *CD* corresponds to the unloading phase of the curve. The absorbed energy E_a was calculated as the difference between the area of work during the loading phase *OC* and the area of work during the unloading phase *CD* in the corresponding force-deformation curve. Considering the region of symptoms, the fruit mechanical damage occurred always near the blossom area resulting from the loading contact between fruit and probe and the stem area resulting from the loading contact between fruit and base (Fig. 3-a2 and a3). The mechanical damage near the blossom area of fruit was always enhanced compared to the stem area of fruit. This can be attributed to the curvature of fruit contour at the blossom providing a small contact area compared to the contact at the stem. This hypothesis is further supported by the absence of any apparent difference in the mechanical damage between two sides of loading contact surfaces at a given compression level when the fruit samples were compressed along their radial axis on the transverse equatorial section (Fig. 3-b2 and b3). During tests, it was observed that some liquids leaked from tissue failure from the border of the contact surface between fruit and probe with the increase of fruit deformation. However, no clear cracks were observed on the fruit surface until the fruit was compressed to 60% deformation along its stem-blossom axis. By comparing the compression force-deformation data with the visible browning tissue on fruit equatorial sections, the elastic and failure deformation ranges of strawberries at two compression directions were obtained which provided an objective basis for extracting elastic and plastic mechanical parameters from the force-deformation curve of fruit at the macroscopic scale.

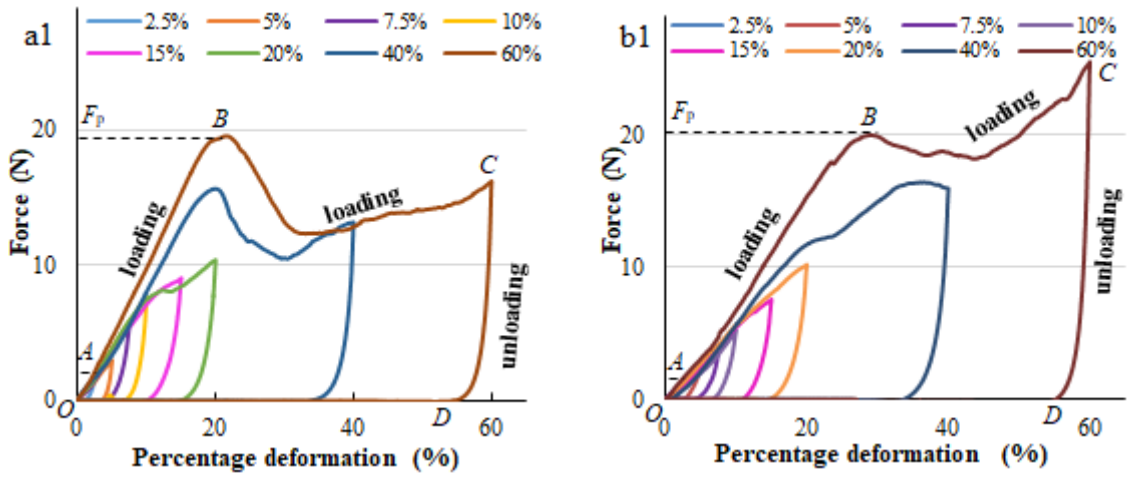

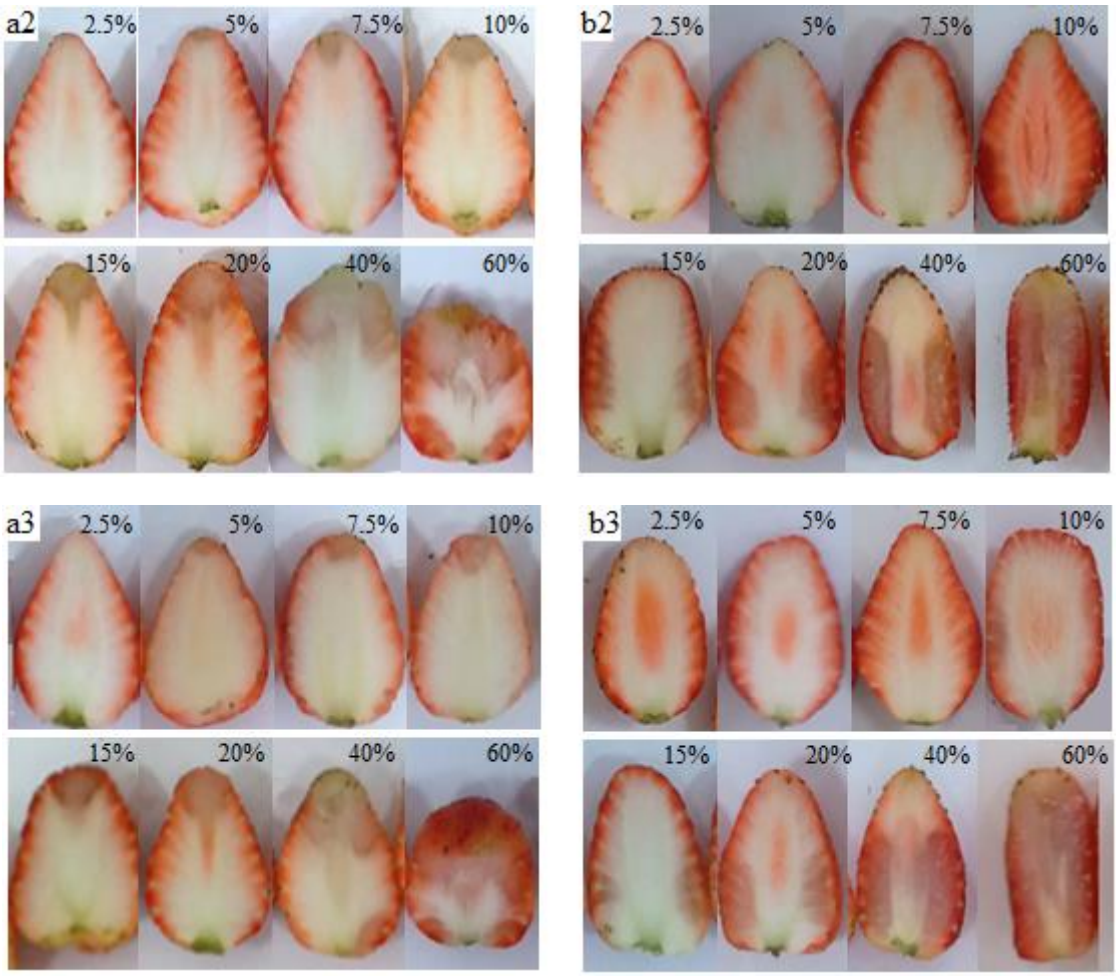

Fig. 3 Typical force-percentage deformation curves and the browning area of strawberry tissues. (a1) eight force-percentage deformation curves loading along the stem-blossom axis at 1 mm/s; (a2 and a3) browning tissues on the longitudinal equatorial section after a fruit was compressed to a given percentage deformation along stem-blossom axis at 1 or 5 mm/s and then stored for 4 h, respectively; (b1) eight force-percentage deformation curves loading along the radial axis at 1 mm/s; (b2 and b3) browning tissues on the longitudinal equatorial section after a fruit was compressed to a given percentage deformation along the radial axis at 1 or 5 mm/s and then stored for 4 h, respectively.

3.2.2 Failure mechanics of whole strawberries

3.2.2.1 Loading slope of the whole fruit

The loading slope of the whole fruit at the elastic deformation stage (percentage deformation < 2.5 %) was weakly affected by the loading direction and compression speed (Fig. 4a). As the fruit was compressed along its stem-blossom axis on the longitudinal equatorial section or radial axis on the transverse equatorial section, the average loading slope at 5 mm/s was always slightly greater than that at 1 mm/s, which could be explained by the theorem of momentum as the fruit will be subjected to a

large compression peak force (corresponding to loading slope) at a rapid loading speed. The assumption made here is that the impulses applied to the fruit for a given elastic deformation are the same at two loading speeds. Similarly, the average loading slope of strawberries compressed along the stem-blossom axis was always lower than that along the radial axis, which can be attributed to fact that strawberry fruit is a long ellipsoid and the curvature of fruit contour at the blossom is much greater than that at the transverse equatorial contour. As a result, there would be more compressed cells along the radial axis than along the stem-blossom axis when the fruit was compressed to 2.5% deformation, and the resistance from the radial axis would be larger than that from the stem-blossom axis.

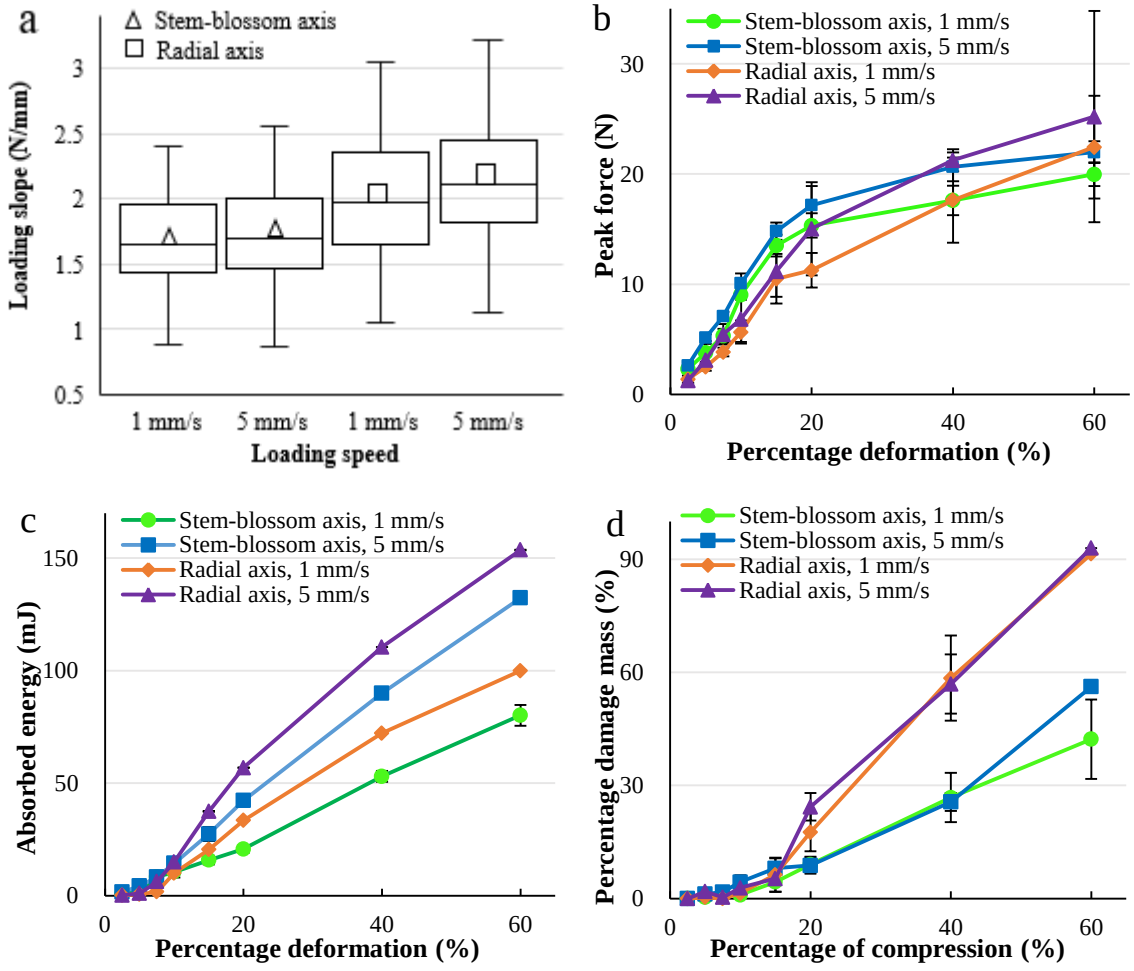

Fig. 4 Mechanical properties of strawberries under compression. (a), (b), (c) and (d) Loading slope, peak force, absorbed energy and percentage damage mass of strawberries at different compression direction (along the stem-blossom axis and radial axis) and loading speed (1 and 5 mm/s) for each percentage deformation.

3.2.2.2 Effect of compressibility level

With the increase of the final percentage deformation of the fruit, the peak force initial increased

rapidly and then slowly (Fig. 4b), which could be attributed to different types of deformation experienced by the fruit before and after the inflection point. Indeed, the fruit surface near the compression position is convex and the contact area between the probe and the fruit surface would gradually increase with the percentage deformation during loading before the fruit structural failure. Likewise, the number of the compressed cells would also gradually increase, and as a result, the fruit might experience an elastic deformation stage and a local plastic deformation stage before inflection point, after which the sample would experience a structural failure deformation. After the inflection point the contact area between the probe and the fruit surface during loading would no longer increase whereas the number of compressed cells would continue to gradually increase with the fruit percentage deformation. This is supported by the slow increase in the absorbed energy and percentage of damaged mass of fruit at the elastic deformation and local plastic deformation stages initially when compared to a rapid increase in their values at the structural failure stage (Fig. 4c, d).

3.2.2.3 Effect of compression speed

The loading speed showed a significant effect on the peak force and absorbed energy ($p<0.05$) but did not have any significant effect on the percentage of damaged mass ($p>0.05$). When the fruit was compressed to a given percentage deformation along its stem-blossom axis on the longitudinal equatorial section or radial axis on the transverse equatorial section, the resulting peak forces and absorbed energies at 5 mm/s were always larger than those at 1 mm/s (Fig. 4b and c). This is probably because the compressed tissue in the fruit experienced a rapid reduction in its bulk volume in a short time when the fruit is compressed quickly to a given percentage deformation. Consequently, the fruit produced high resistance i.e. high peak force to the top-loading probe, based on the theorem of momentum with an assumption that the impulses applied to fruits are same at 1 and 5 mm/s. For the same reason the area of work between loading and unloading phases which correspond to the absorbed energy was relatively larger at a fast loading speed. However, the difference in the peak force and absorbed energy between the two loading speeds gradually became more and more significant with the increasing percentage deformation of fruits (Fig. 4b and c). The obtained results could be explained by the convex fruit surface, especially at the loading positions. Indeed, because the upper surface of the strawberry fruit is convex, the rate of increase in the number of compressed cells in the fruit would gradually improve with the increasing fruit percentage deformation. Furthermore a more rapid compression causes a higher peak force applied to these compressed cells resulting in a growing

difference in the peak force (Fig. 4b) and absorbed energy (Fig. 4c) between fruits compressed at 1 and 5 mm/s. Considering the risk of mechanical damage to the fruit, these results illustrated thresholds of mechanical load that needs to be considered during manual handling, mechanical harvesting, grading, packaging and transportation for while maintaining the fruit's quality.

3.2.2.4 Effect of compression direction

The compression direction showed a significant effect on the peak force, absorbed energy and percentage of damaged mass (p<0.05). Fruit compressed at 1 or 5 mm/s along its stem-blossom axis on the longitudinal equatorial section showed larger peak forces at percentage deformation below 40% when compared to those obtained from a compression along its radial axis on the transverse equatorial section (Fig. 4b). Opposite results were obtained at percentage deformation above 40%. The similar trends were observed for the absorbed energy and percentage of damaged mass which were higher at low percentage deformation and lower at high percentage deformation for compressed fruit along its stem-blossom axis than those of fruit compressed along its radial axis (Fig. 4c and d). These findings could be explained by the shape and structural arrangement of the strawberry fruit which could be considered as a long ellipsoid with a specific structural distribution of inner and outer tissues as shown in Fig. 2a. The inner tissues (e.g., pith, columella) accounts for the main part of the fruit where it is distributed along the stem-blossom axis on the longitudinal equatorial section with one side extends to the fruit stem and the other side connects the outer tissues. Conversely, the outer tissues (e.g., exocarp and mesocarp) mainly cover the inner tissues of the fruit from its top. In addition to the asymmetric distribution of the inner and outer tissues along the stem-blossom axis, the inner tissues were found to be firmer than the outer tissues, which was confirmed in the presented study. Although at the initial compression stage the probe firstly contacts the outer tissues, it would rapidly apply forces to the firm inner tissues when the loading is along the stem-blossom axis because of the thin layer of the outer tissues near the fruit blossom. When the loading is along the radial axis on the fruit transverse equatorial section the probe mainly applies forces to the soft outer tissues. Hence, when the fruit was at the elastic and local plastic deformation stages during compression, the peak force was high for loading forces along the fruit' stem-blossom as compared to that resulted from the loading along its radial axis. Moreover, because the fruit is a long ellipsoid the curvature of fruit contour at the blossom would be much greater than that at the transverse equatorial contour. These results indicate that strawberries are more susceptible to mechanical damage when the applied load is along their

386 stem-blossom axis and the deformation percentage corresponding to the elastic and local plastic
387 deformation stages. The damage mainly occurred near the fruit's blossom (Fig. 4d) and the absorbed
388 energy is higher than that from the loading along the radial axis (Fig. 4c). With further increase in the
389 fruit percentage deformation, whether the loading is along the stem-blossom axis or radial axis the
390 probe would apply forces to the firm inner tissues because of the broken outer tissues. Because
391 strawberry is a long ellipsoidal fruit, its firm inner tissues (e.g., pith, columella) approximate a long
392 irregular solid along the fruit stem-blossom axis and the probe would compress the narrow end when
393 the loading is along the stem-blossom axis whereas the probe would compress the broadside when the
394 loading is along the radial axis. As a result, strawberries subjected to a loading force along their radial
395 axis showed higher resistance (corresponding to peak force), absorbed energy and percentage of
396 damaged mass when compared to those subjected to a loading along their stem-blossom axis (Fig. 4).
397 These findings suggest that fresh strawberries could be fixed along their stem-blossom axis and
398 vertically placed in pack cases to avoid their surface to be subjected to loading forces during
399 packaging and transporting.

400 **3.2.3 Correlations between fruit mechanical parameters**

401 The Pearson correlation coefficients between the mechanical parameters of strawberries are
402 presented in Table 2. This shows that there was a high positive linear correlation between experimental
403 values of peak force and absorbed energy and between absorbed energy and percentage of damaged
404 mass of fruits subjected to loading forces along their stem-blossom axis and radial axis at 1 or 5 mm/s.
405 Similar results were found by Sirisomboon et al. (2012) and Li et al. (2015) for tomato fruits,
406 Pérez-López et al. (2014) for peach, and Liu et al. (2019) for apple. These Pearson correlation
407 coefficients between fruit mechanical parameters varied to some extent with the loading conditions,
408 such as loading speed and compression directions. There was stronger correlation between absorbed
409 energy and percentage of damaged mass (coefficient of determination, more than 0.95). This result
410 indicates that the percentage of damaged mass of strawberries could be better predicted from the
411 absorbed energy. This is a particularly useful finding as evaluating the percentage of damaged mass is
412 a tedious process and challenging to accurately measure whereas the absorbed energy is easily
413 measured by loading-unloading tests.

414 **Table 2** Pearson correlation coefficient between mechanical parameters of fruits at two loading speeds,
415 and two loading directions

Correlation	Loading along the stem-blossom axis		Loading along the radial axis	
	1 mm/s	5 mm/s	1 mm/s	5 mm/s
F_p - E_a	0.85 (p<0.0001)	0.88 (p<0.0001)	0.94 (p<0.0001)	0.89 (p<0.0001)
R- F_p	0.79 (p<0.0001)	0.78 (p<0.0001)	0.89 (p<0.0001)	0.84 (p<0.0001)
E_a - R	0.95 (p<0.0001)	0.97 (p<0.0001)	0.98 (p<0.0001)	0.98 (p<0.0001)

Note: F_p - E_a indicates the correlation between peak force and absorbed energy; R- F_p indicates the correlation between percentage of damaged mass and peak force; E_a - R indicates the correlation between absorbed energy and percentage of damaged mass.

Fruit mechanical damage is the failure of a biomaterial, and as such closely relates to fruit mechanics (Li and Thomas, 2014). Hence, quantitatively characterizing the mechanical damage of strawberry fruits using one of the easily-measured mechanical parameters, such as absorbed energy would be an effective method. It is worth noted that the mass loss of the damaged tissue is a relative slow and hysteresis physiological process during storage, otherwise the correlation between absorbed energy and percentage of damaged mass could have been even stronger.

3.3 Failure mechanical properties of strawberry tissues

3.3.1 Loading-unloading tests

The loading-unloading tests at 1, 3 and 5 mm/s were performed on strawberry outer and inner tissue samples with similar dimensions, about 11 mm, length × 11 mm, width × 18 mm thickness (Table 3). The samples were divided into six groups and the data in each column represented the average values ± standard deviations of each sample group (tissue type × loading speed). Again, as in the case of the whole fruit, the six groups were similar with respect to the initial length, width and thickness according to multivariate ANOVA (Table 3). Therefore, bias in data obtained by the loading-unloading tests due to the sample geometry associated with each loading speed test group was minimized.

Table 3 Geometric sizes of strawberry tissue samples

Parameters	Outer tissue			Inner tissue		
	1 mm/s	3 mm/s	5 mm/s	1 mm/s	3 mm/s	5 mm/s
L, mm	10.8±0.3[a]	11.1±0.2[a]	11.0±0.2[a]	11.3±0.3[a]	11.1±0.3[a]	10.9±0.5[a]

w, mm	11.4±0.2[a]	10.9±0.4[a]	10.8±0.4[a]	11.0±0.2[a]	11.2±0.3[a]	10.9±0.6[a]
d, mm	17.9±0.3[a]	17.8±1.2[a]	18.1±0.6[a]	18.0±1.2[a]	17.9±0.2[a]	1.84±0.5[a]

Note: Data are expressed as the mean ± standard deviation (n = 5). Different superscript letters (namely a, b) in the same row indicate significant difference ($p < 0.05$) according to ANOVA. *L*, *w* and *d* - the initial length, width and thickness of strawberry fruit tissue samples, respectively.

Typical force-percentage deformation curves for compression test of strawberry outer and inner tissues to 50% at 1, 3 and 5 mm/s are presented in Fig. 5. Taking the force-percentage deformation curves at 5 mm/s as an example, each curve included a loading phase *OPQ* and an unloading phase *QS*. An abrupt decrease in loading force in the loading phase when the tissue sample failure was observed. The elastic peak force F_{cmax} is the force at the first significant peak point *P* during loading phase and corresponds to the beginning of the tissue failure. Hence, the failure stress of each tissue could be inferred from the ratio of the elastic peak force F_{cmax} to the cross-sectional area A_c of the tissue sample. Similarly, the compression elastic modulus of each tissue could be inferred from the ratio of the failure stress σ_c to its strain ε_c (Alamar et al., 2008). The failure energy E_{rec} was measured as the area of work during the loading phase of the corresponding force-deformation curve before the tissue failure (Link et al., 2018).

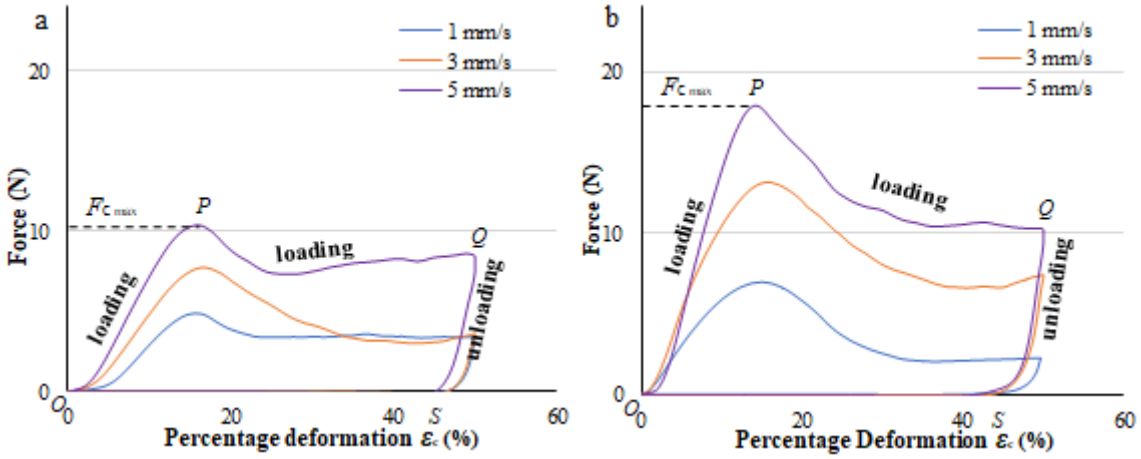

Fig.5 Typical loading-unloading curves for compression test of strawberry tissues to 50% at different compression speeds. (a) Loading-unloading curves of strawberry outer tissues at 1, 3 and 5 mm/s, respectively; (b) Loading-unloading curves of strawberry inner tissues at 1, 3 and 5 mm/s, respectively.

3.3.2 Failure mechanics of strawberry tissues

3.3.2.1 Effect of tissue type

The failure mechanical properties of strawberry outer and inner tissues at the three loading speeds of 1, 3, 5 mm/s are listed in Table 4. The results of multivariate analysis of variance (MANOVA) indicated a significant effect of the type of tissue (e.g., outer and inner tissues) on the failure stress σ_c, failure strain ε_c, failure energy E_{rec} and compression elastic modulus E_c of strawberry tissues ($p<0.05$). The results of multiple comparisons in MANOVA showed that the average failure stress, failure strain, failure energy and compression elastic modulus of strawberry inner tissues were 0.093 MPa, 17.7%, 8.09 mJ, 0.53 MPa, which was 1.27, 1.14, 1.47, 1.15 times significantly higher than those of outer tissues ($p<0.05$), respectively. These findings could be attributed to the differences in the size, type and chemical component of cells present in these two kinds of tissues alongside different arrangement between vascular tissues and different types of cells. In this study, the obtained outer tissues mainly included cortical cells, hypodermal cells and vascular tissues while the obtained inner tissues mainly included hypodermal cells, pith cells and vascular tissues. Pectin content gradually decreases from hypodermis to cortex tissues whereas from vascular to cortical tissues the protein and carbohydrate content also gradually decrease (Suutarinen et al., 1998). From the outer cortical tissues to the inner hypodermis, cells shape change from irregular to approximately spherical. Likewise, cells gradually increase in size and the porosity between adjacent cells become bigger (Contigiani et al., 2018). Additionally, there are apparent differences in the orientation of vascular bundles in the outer and inner tissues (Suutarinen et al., 1998; Suutarinen et al., 2000). De Bruijn et al. (2016) and Duarte-Molina et al. (2016) reported that the puncture elastic modulus of strawberry tissues approximated 0.33 and 0.011 MPa, respectively. These values are lower than those of compression elastic modulus of strawberry outer and inner tissues from this study. The reason might be that the friction force on the sides of the puncture probe reduces the normal compression force during puncturing (Grotte et al., 2001).

In summary, the outer tissues in a strawberry fruit are more susceptible to mechanical damage than the inner tissues. Conversely, the failure stress, failure strain and elastic modulus of the outer green rind in watermelon tissues were 1.23 MPa, 26.6%, 4.94 MPa, which was 45.56, 5.12, 9.21 times significantly higher than those of the inner red flesh tissues, respectively (Sadrnia et al., 2008). Similarly, the failure stress of peel grapefruit was 0.47 MPa and 6.71 times higher than of the pulp tissues (Miraei Ashtiani et al., 2019). All these findings demonstrate the difference in the failure

mechanics between different types of fruits.

Table 4 Failure mechanical properties of strawberry outer and inner tissue samples

Samples	Loading speed (mm/s)	Mechanical parameters			
		$\boldsymbol{\sigma_c}$ (MPa)	$\boldsymbol{\varepsilon_c}$ (%)	$\boldsymbol{E_{rec}}$ (mJ)	$\boldsymbol{E_c}$ (MPa)
Outer tissue	1	0.059±0.002	16.6±1.64	3.73±0.11	0.36±0.03
	3	0.076±0.004	15.4±1.27	5.70±0.31	0.44±0.03
	5	0.085±0.012	14.7±2.67	7.06±0.99	0.58±0.04
Inner tissue	1	0.076±0.005	18.4±2.84	5.68±0.45	0.42±0.03
	3	0.090±0.034	17.6±0.22	7.96±3.05	0.51±0.19
	5	0.114±0.019	17.1±0.48	10.62±1.81	0.66±0.10

Note: Data are expressed as the mean ± standard deviation (n = 5). σ_c, ε_c, E_{re} and E_c - the failure stress, failure strain, failure energy and compression elastic modulus of strawberry tissue samples, respectively.

3.3.2.2 Effect of loading speed

The results of multivariate analysis of variance (MANOVA) showed a significant effect of the loading speed (e.g., 1, 3 and 5 mm/s) on the failure stress σ_c, failure energy E_{rec} and compression elastic modulus E_c of strawberry tissues (p<0.05). However, the failure strain of strawberry tissues did not significantly depend on the loading speed, indicating that the strawberry tissues approximate brittle biomaterial, which is similar to the analysis on bovine liver by Lu et al. (2014). The failure stress, failure energy and compression elastic modulus gradually increased with the increasing loading speed. The average failure stress, failure energy and compression elastic modulus of strawberry tissues at 5 mm/s were 0.099 MPa, 8.84 mJ, 0.62 MPa, which were 1.48, 1.88, 1.61 times significantly higher than those obtained at 1 mm/s (p<0.05), respectively. Similar increase in these failure mechanical parameters with increasing compression speed have been found by Kohyama et al. (2013) on cucumber tissues. The results could be explained by the change in turgor pressure in fruit tissue cells under different compression speeds. The cell turgor pressure is the force exerted on the cell membrane by the intracellular fluid and its osmotic potential (Duarte-Molina et al., 2016) and its value is 0 when no stress is applied to an intact tissue (Singh et al., 2014). When a tissue is compressed at various speeds, the cells in the tissue produce different turgor pressures and low speed would allow some intracellular fluids in single cells to have enough time for flowing out from each cells. Although

strawberry tissues under high-speed compression showed large failure mechanical parameters and superficially seems insusceptible to produce immediately mechanical damage, the hysteresis damage of the strawberry tissues under high-speed compression was more serious than that under low-speed compression. Hence, from farms to markets a series of slow and gentle handlings are vital for fresh fruits to maintain high quality.

4. Conclusion

Textural failure mechanics of strawberry fruits and their tissues were characterized by loading-unloading tests at different compression speeds. Strawberry fruit showed expected three stages of deformation during loading phase, namely elastic, local plastic and structural failure deformation. Their cut-off points depended on the compression speed and loading direction, which was further validated by the corresponding visible browning processes in tissues from fruit longitudinal equatorial section. The peak force and absorbed energy depended on the loading direction and compression speed whereas the percentage damaged mass only depended on the loading direction. The fruit was most susceptible to mechanical damage when it was compressed along its stem-blossom axis at low percentage deformation and along its radial axis at high percentage deformation. A strong correlation was found between the absorbed energy and percentage damaged mass of the fruit, despite the relative slow and hysteresis physiological process of mass loss in damaged tissue during storage. This result suggests that the absorbed energy could be an appropriate and easily measurable mechanical parameter for quantitatively assessing the degree of fruit damage.

The average failure stress, failure strain, failure energy and elastic modulus of fruit inner tissues were 0.093 MPa, 17.7%, 8.09 mJ, 0.53 MPa, which was 1.27, 1.14, 1.47, 1.15 times enhanced compared to values of outer tissues ($p<0.05$), respectively. Hence the outer tissues in a strawberry fruit are more susceptible to mechanical damage than the inner tissues. Although the failure stress, failure energy and elastic modulus of strawberry tissues were increased by the compression speed, the hysteresis damage of strawberry tissue under high-speed compression was more serious than that under low-speed compression. Therefore, from farms to markets a series of slow and gentle handlings are vital for fresh fruits to maintain high quality. The obtained tissue mechanics could be used to non-destructively and quantitatively predict the internal mechanical damage evolution and damage volume changing of strawberries by numerical simulation. These findings would contribute the pool of information required for the development more efficient and effective harvesting robot whereas the

failure mechanical evaluation method might also be used for other living plant materials.

Acknowledgements: This work was supported by a European Marie Curie International Incoming Fellowship (326847 and 912847), a Special Foundation for Talents of Northwest A&F University (Z111021801), two Key Research and Development Plan of Shaanxi Province (2019NY-172 and 2019TSLNY01-01) and a Project for Sino-German Cooperation on Agricultural Science and Technology in 2018-2019 (15).

References

Alamar, M.C., Vanstreels, E., Oey, M.L., Moltó, E., Nicolaï, B.M., (2008). Micromechanical behaviour of apple tissue in tensile and compression tests: Storage conditions and cultivar effect. Journal of Food Engineering 86(3), 324-333.

Aliasgarian, S., Ghassemzadeh, H.R., Moghaddam, M., Ghaffari, H., (2015). Mechanical damage of strawberry during harvest and postharvest operations. Acta Technologica Agriculturae 18(1), 1-5.

Bovi, G.G., Caleb, O.J., Ilte, K., Rauh, C., Mahajan, P.V., (2018). Impact of modified atmosphere and humidity packaging on the quality, off-odour development and volatiles of '*Elsanta*' strawberries. Food Packaging and Shelf Life 16, 204-210.

Chaiwong, S., Bishop, C.F., (2015). Effect of vibration damage on the storage quality of '*Elsanta*' strawberry. Australian Journal of Crop Science 9(9), 859-864.

Chaves, V.C., Calvete, E., Reginatto, F.H., (2017). Quality properties and antioxidant activity of seven strawberry (*Fragaria x ananassa* duch) cultivars. Scientia Horticulturae 225, 293-298.

Contigiani, E.V., Jaramillo-Sánchez, G., Castro, M.A., Gómez, P.L., Alzamora, S.M., (2018). Postharvest quality of strawberry fruit (*Fragaria x ananassa* duch *Cv*. *Albion*) as affected by Ozone washing: Fungal spoilage, mechanical properties, and structure. Food and Bioprocess Technology 11(9), 1639-1650.

De Bruijn, J., Rivas, F., Rodriguez, Y., Loyola, C., Flores, A., Melin, P., Borquez, R., (2016). Effect of vacuum microwave drying on the quality and storage stability of strawberries. Journal of Food Processing and Preservation 40(5), 1104-1115.

Dieter Fischer, W.C., B. Hunt Ashby, (1990). Reducing transportation damage to grapes and strawberries. Journal of Food Distribution Research, 193-202.

Duarte-Molina, F., Gómez, P.L., Castro, M.A., Alzamora, S.M., (2016). Storage quality of strawberry fruit treated by pulsed light: Fungal decay, water loss and mechanical properties. Innovative Food

568 Science & Emerging Technologies 34, 267-274.
569 FAOSTAT, (2019). Food and Agriculture Organization of the United Nations. Available from:
570 http://www.fao.org/faostat/zh/#data/QC.
571 Grotte, M., Duprat, F., Loonis, D., Pietri, E., (2001). Mechanical properties of the skin and the flesh
572 apple. International Journal of Food Properties 4, 149-161.
573 Jahanbakhshi, A., Abbaspour-Gilandeh, Y., Gundoshmian, T.M., (2018). Determination of physical
574 and mechanical properties of carrot in order to reduce waste during harvesting and post-harvesting.
575 Food Science & Nutrition 6(7), 1898-1903.
576 Ji, W., Qian, Z., Xu, B., Tang, W., Li, J., Zhao, D., (2017). Grasping damage analysis of apple by
577 end-effector in harvesting robot. Journal of Food Process Engineering 40(6), e12589.
578 Kelly, K., Madden, R., Emond, J.P., Do Nascimento Nunes, M.C., (2019). A novel approach to
579 determine the impact level of each step along the supply chain on strawberry quality. Postharvest
580 Biology and Technology 147, 78-88.
581 Kohyama, K., Kato-Nagata, A., Shimada, H., Kazami, Y., Hayakawa, F., (2013). Texture of sliced
582 cucumbers measured by subjective human-bite and objective instrumental tests. Journal of Texture
583 Studies 44(1), 1-11.
584 La Scalia, G., Aiello, G., Miceli, A., Nasca, A., Alfonzo, A., Settanni, L., (2016). Effect of vibration on
585 the quality of strawberry fruits caused by simulated transport. Journal of Food Process Engineering
586 39(2), 140-156.
587 Li, Z., (2013). The effect of compressibility, loading position and probe shape on the rupture
588 probability of tomato fruits. Journal of Food Engineering 119(3), 471-476.
589 Li, Z., Andrews, J., Wang, Y., (2017a). Mathematical modelling of mechanical damage to tomato fruits.
590 Postharvest Biology and Technology 126, 50-56.
591 Li, Z., Li, P., Yang, H., Liu, J., Xu, Y., (2012). Mechanical properties of tomato exocarp, mesocarp and
592 locular gel tissues. Journal of Food Engineering 111(1), 82-91.
593 Li, Z., Lv, K., Wang, Y., Zhao, B., Yang, Z., (2015). Multi-scale engineering properties of tomato fruits
594 related to harvesting, simulation and textural evaluation. LWT - Food Science and Technology 61(2),
595 444-451.
596 Li, Z., Miao, F., Andrews, J., (2017b). Mechanical models of compression and impact on fresh fruits.
597 Comprehensive Reviews in Food Science and Food Safety 16(6), 1296-1312.

598 Li Z., Miao F., Yang Z, Chai P., Yang S., (2019). Factors affecting human hand grasp type in tomato
599 fruit-picking: A statistical investigation for ergonomic development of harvesting robot. Computers
600 and Electronics in Agriculture 157, 90-97.
601 Li, Z., Thomas, C., (2014). Quantitative evaluation of mechanical damage to fresh fruits. Trends in
602 Food Science & Technology 35(2), 138-150.
603 Liang Z., Xu L., Baerdemaeker J., Li Y., Saeys W., (2020). Optimisation of a multi-duct cleaning
604 device for rice combine harvesters utilising CFD and experiments. Biosystems Engineering 190,
605 25-40.
606 Link, J.V., Tribuzi, G., Oliveira de Moraes, J., Laurindo, J.B., (2018). Assessment of texture and
607 storage conditions of mangoes slices dried by a conductive multi-flash process. Journal of Food
608 Engineering 239, 8-14.
609 Liu, S., Yang, H., Bian, Z., Tao, R., Chen, X., Lu, T., (2019). Regulation on mechanical properties of
610 spherically cellular fruits under osmotic stress. Journal of the Mechanics and Physics of Solids 127,
611 182-190.
612 Lu, Y.C., Kemper, A.R., Untaroiu, C.D., (2014). Effect of storage on tensile material properties of
613 bovine liver. Journal of the Mechanical Behavior of Biomedical Materials 29, 339-349.
614 Mahalik, Nitaigour, (2014). Advances in packaging methods, processes and systems. Challenges 5(2),
615 374-389.
616 Miraei Ashtiani, S.H., Sadrnia, H., Mohammadinezhad, H., Aghkhani, M.H., Khojastehpour, M.,
617 Abbaspour-Fard, M.H., (2019). FEM-based simulation of the mechanical behavior of grapefruit under
618 compressive loading. Scientia Horticulturae 245, 39-46.
619 Ornelas-Paz, J.d.J., Yahia, E.M., Ramírez-Bustamante, N., Pérez-Martínez, J.D., Escalante-Minakata,
620 M.d.P., Ibarra-Junquera, V., Acosta-Muniz, C., Guerrero-Prieto, V., Ochoa-Reyes, E., (2013). Physical
621 attributes and chemical composition of organic strawberry fruit (*Fragaria x ananassa* duch, *Cv. Albion*)
622 at six stages of ripening. Food Chemistry 138(1), 372-381.
623 Pérez-López, A., Chávez-Franco, S.H., Villaseñor-Perea, C.A., Espinosa-Solares, T.,
624 Hernández-Gómez, L.H., Lobato-Calleros, C., (2014). Respiration rate and mechanical properties of
625 peach fruit during storage at three maturity stages. Journal of Food Engineering 142, 111-117.
626 Pham, Q.T., Liou, N.S., (2017). Investigating texture and mechanical properties of *Asian* pear flesh by
627 compression tests. Journal of Mechanical Science & Technology 31(8), 3671-3674.

628 Sadrnia, H., Rajabipour, A., Jafari, A., Javadi, A., Mostofi, Y., Kafashan, J., Dintwa, E., De
629 Baerdemaeker, J., (2008). Internal bruising prediction in watermelon compression using nonlinear
630 models. Journal of Food Engineering 86(2), 272-280.
631 Singh, F., Katiyar, V.K., Singh, B.P., (2014). Analytical study of turgor pressure in apple and potato
632 tissues. Postharvest Biology and Technology 89, 44-48.
633 Sirisomboon, P., Tanaka, M., Kojima, T., (2012). Evaluation of tomato textural mechanical properties.
634 Journal of Food Engineering 111(4), 618-624.
635 Stopa, R., Szyjewicz, D., Komarnicki, P., Kuta, L., (2018). Determining the resistance to mechanical
636 damage of apples under impact loads. Postharvest Biology and Technology 146, 79-89.
637 Suutarinen, J., Änäkäinen, L., Autio, K., (1998). Comparison of light microscopy and spatially
638 resolved fourier transform infrared (ft-ir) microscopy in the examination of cell wall components of
639 strawberries. LWT - Food Science and Technology 31(7), 595-601.
640 Suutarinen, J., Heiska, K., Moss, P., Autio, K., (2000). The effects of Calcium chloride and sucrose
641 prefreezing treatments on the structure of strawberry tissues. LWT - Food Science and Technology
642 33(2), 89-102.
643 Tang Z., Li Y., Li X., Xu T., (2019). Structural damage modes for rice stalks undergoing threshing.
644 Biosystems Engineering 186, 323-336.
645 Yan, J., Luo, Z., Ban, Z., Lu, H., Li, D., Yang, D., Aghdam, M.S., Li, L., (2019). The effect of the
646 layer-by-layer (LBL) edible coating on strawberry quality and metabolites during storage. Postharvest
647 Biology and Technology 147, 29-38.
648 Zeliou, K., Papasotiropoulos, V., Manoussopoulos, Y., Lamari, F.N., (2018). Physical and chemical
649 quality characteristics and antioxidant properties of strawberry cultivars (*Fragaria* × *ananassa* duch.)
650 in Greece: assessment of their sensory impact. Journal of the Science of Food and Agriculture 98(11),
651 4065-4073.
652 Zhang, C., Li, W., Zhu, B., Chen, H., Chi, H., Li, L., Qin, Y., Xue, J., (2018). The quality evaluation of
653 postharvest strawberries stored in Nano-Ag packages at refrigeration temperature. Polymers 10, 1-17.
654 Zhuang, J., Hou C.,, Tang Y., He Y., Guo Q., Zhong Z., Luo S., (2019). Computer vision-based
655 localisation of picking points for automatic litchi harvesting applications towards natural scenarios.
656 Biosystems Engineering 187, 1-20.
657 Zhuang, J., Luo S., Hou C., Tang Y., He Y., Xue X., (2018). Detection of orchard citrus fruits using a

658 monocular machine vision-based method for automatic fruit picking applications. Computers and
659 Electronic in Agriculture 152, 64-73.
660 Zude, M., Hashim, N., Hass, R., Polley, N., Regen, C., (2019). Validation study for measuring
661 absorption and reduced scattering coefficients by means of laser-induced backscattering imaging.
662 Postharvest Biology and Technology 153, 161-168.
663 Zude, M., Herold, B., Roger, J.-M., Bellon-Maurel, V., Landahl, S., (2006). Non-destructive tests on
664 the prediction of apple fruit flesh firmness and soluble solids content on tree and in shelf life. Journal
665 of Food Engineering 77(2), 254-260.
666